



Title	Are males just passive? Coupling mechanism of the Brazilian cave insects with inverted genitalia
Author(s)	Cheng, Zixin; Kamimura, Yoshitaka; Ferreira, Rodrigo L.; Lienhard, Charles; Yoshizawa, Kazunori
Citation	Science of nature, 110 <a href="https://doi.org/10.1007/s00114-023-01855-8">https://doi.org/10.1007/s00114-023-01855-8</a>
Issue Date	2023-06-01
Doc URL	<a href="http://hdl.handle.net/2115/92524">http://hdl.handle.net/2115/92524</a>
Rights	This version of the article has been accepted for publication, after peer review (when applicable) and is subject to Springer Nature 's AM terms of use, but is not the Version of Record and does not reflect post-acceptance improvements, or any corrections. The Version of Record is available online at: <a href="http://dx.doi.org/10.1007/s00114-023-01855-8">http://dx.doi.org/10.1007/s00114-023-01855-8</a>
Type	article (author version)
File Information	2023_NAWI.pdf



[Instructions for use](#)

1 **Are males just passive? Coupling mechanism of the Brazilian cave insects with**  
2  
3 **inverted genitalia**

4  
5  
6 3

7  
8 4 Zixin Cheng<sup>1, 2</sup>, Yoshitaka Kamimura<sup>3</sup>, Rodrigo L. Ferreira<sup>4</sup>, Charles Lienhard<sup>5</sup> and  
9  
10 5 Kazunori Yoshizawa<sup>1</sup>

11  
12  
13  
14 6 <sup>1</sup>. Systematic Entomology, School of Agriculture, Hokkaido University, Sapporo 060-8589, Japan

15  
16  
17 7 <sup>2</sup> State Key Laboratory of Freshwater Ecology and Biotechnology, Institute of Hydrobiology,  
18  
19  
20  
21 8 Chinese Academy of Sciences, Wuhan 430072, China

22  
23  
24 9 <sup>3</sup>. Department of Biology, Keio University, Yokohama 223-8521, Japan

25  
26  
27  
28 10 <sup>4</sup>. Department of Ecology and Conservation, Federal University of Lavras, CEP 37200-900 Lavras  
29  
30 11 (MG), Brazil

31  
32  
33 12 <sup>5</sup>. Geneva Natural History Museum, CP 6434, 1211 Geneva 6, Switzerland

34  
35  
36  
37 13 Correspondances

38  
39  
40 14 Zixin Cheng

41  
42  
43 15 [zixin@ihb.ac.cn](mailto:zixin@ihb.ac.cn)

44  
45  
46 16 Kazunori Yoshizawa

47  
48  
49 17 [psocid@agr.hokudai.ac.jp](mailto:psocid@agr.hokudai.ac.jp)

50  
51  
52  
53  
54 18

55  
56  
57 19 **Abstract**

58  
59  
60 20 Species of the Brazilian cave barklouse genus *Neotrogla* (Psocodea: “Psocoptera”:

1  
2  
3  
4  
5  
6  
7  
8  
9  
10  
11  
12  
13  
14  
15  
16  
17  
18  
19  
20  
21  
22  
23  
24  
25  
26  
27  
28  
29  
30  
31  
32  
33  
34  
35  
36  
37  
38  
39  
40  
41  
42  
43  
44  
45  
46  
47  
48  
49  
50  
51  
52  
53  
54  
55  
56  
57  
58  
59  
60  
61  
62  
63  
64  
65

1 21 Trogiomorpha: Prionoglarididae: Sensitibillini) are known to have a “female penis  
2  
3 22 (gynosome)” that functions as an intromittent organ inserted into the membranous  
4  
5  
6 23 pouches in the simple male genital chamber during copulation to receive semen.  
7  
8  
9 24 However, the functions of other male and female genital structures and the copulatory  
10  
11 25 processes of *Neotroglia* were completely unknown to date. Based on  $\mu$ CT observation  
12  
13  
14 26 of the male and female postabdomen and connected muscles both before and in copula,  
15  
16  
17 27 we clarified the functions of the male and female genital structures. In addition, based  
18  
19  
20 28 on the analyses of the established 3D models, we concluded that precise and rigid  
21  
22  
23 29 contact of multiple genital structures, and step-by-step releases of each holding  
24  
25  
26 30 mechanism achieved by the cooperation of both sexes are involved in the copulatory  
27  
28  
29 31 processes. The coevolution between the male and female genital structures in *Neotroglia*  
30  
31 32 may provide a new example for the evolution of tolerance traits.

33

34

35 **Keywords**

36 genitalia, copulatory processes, sexual selection, muscles

37

38

39

40

41

42

1  
2  
3  
4  
5  
6  
7  
8  
9  
10  
11  
12  
13  
14  
15  
16  
17  
18  
19  
20  
21  
22  
23  
24  
25  
26  
27  
28  
29  
30  
31  
32  
33  
34  
35  
36  
37  
38  
39  
40  
41  
42  
43  
44  
45  
46  
47  
48  
49  
50  
51  
52  
53  
54  
55  
56  
57  
58  
59  
60  
61  
62  
63  
64  
65

1       43    **Introduction**

2  
3       44    The Brazilian cave insect genus *Neotrogl* (Psocodea: Trogiomorpha: Prionoglarididae:  
4  
5       45    Sensitibillini) has been receiving much attention since it was discovered that the  
6  
7       46    females have a penis-like intromittent structure called gynosome (Lienhard *et al.*, 2010).  
8  
9       47    The gynosome, generally known as a female penis, is inserted into a vagina-like male  
10  
11       48    structure during copulation to obtain semen (Yoshizawa *et al.*, 2014). The female penis  
12  
13       49    has also been found in the African genus *Afrotrogl* (Lienhard, 2007). Both *Neotrogl*  
14  
15       50    and *Afrotrogl* belong to the small tribe Sensitibillini, containing three genera and  
16  
17       51    eleven named species only, and the well-developed female penis is considered to have  
18  
19       52    evolved independently in these two genera (Yoshizawa *et al.*, 2018b; Cheng *et al.*, 2023).  
20  
21       53    In recent years, several in-depth studies have been conducted on the factors affecting  
22  
23       54    the formation of female intromittent structures, such as the oligotrophic environment,  
24  
25       55    male nuptial gifts, female multiple sperm storage, female-above copulating position,  
26  
27       56    elongated spermathecal duct, and the absence of male penetrative genitalia (Yoshizawa  
28  
29       57    *et al.*, 2014, 2018ab, 2019; Kamimura *et al.*, 2021).

30  
31       58        All these studies focused on the intromittent female penis, but the morphology and  
32  
33       59    function of other genital structures in these sex-reversed insects are still poorly  
34  
35       60    understood. Referring to muscle homology, Cheng *et al.* (2023) determined that the  
36  
37       61    female penis evolved from the spermapore plate, and its unique intromittent function is  
38  
39       62    brought by two pairs of novel muscles formed only within the Sensitibillini. Are there  
40  
41       63    novel structures and muscles in the other genital structures? What functions do other  
42  
43       64    genital structures have during copulation? Do females copulate coercively, and are  
44  
45  
46  
47  
48  
49  
50  
51  
52  
53  
54  
55  
56  
57  
58  
59  
60  
61  
62  
63  
64  
65

1 65 males just passive for mating? What types of sexual selection are strongly reflected in  
2  
3 66 the copulatory processes? All these questions need to be answered under the overall  
4  
5  
6 67 grasp of the structures of male and female genitalia and the copulatory processes of  
7  
8  
9 68 these cave insects with inverted genitalia.

10  
11 69 In this study, by using the synchrotron  $\mu$ CT technique, we present 3D models of  
12  
13  
14 70 the whole male and female genital structures and their associated muscles of *Neotrogl*  
15  
16  
17 71 *curvata*. By comparing the morphological changes of the genital structures and  
18  
19  
20 72 associated muscles before and during copulation, we clarify the functions of these  
21  
22  
23 73 structures and estimate the complete copulatory processes. We also analysed the  
24  
25  
26 74 homology of the muscles between *Neotrogl*a species and the other non-genital-reversed  
27  
28 75 Psocodea and traced the origin of each structure and muscle of *Neotrogl*a.

29  
30  
31 76

## 32 33 34 77 **Materials and Methods**

35  
36 78 A copulating pair and a noncopulating male and female of the coupling-role reversed  
37  
38  
39 79 cave psocid *Neotrogl*a *curvata* Lienhard & Ferreira, 2013 (Trogomorpha) were  
40  
41  
42 80 examined. A noncopulating male and female of *N. brasiliensis* Lienhard, 2010  
43  
44  
45 81 (Lienhard et al., 2010) and noncopulating male specimens of *Trichadenotecnum*  
46  
47  
48 82 *pseudomedium* Yoshizawa, 2001 (Psocomorpha: Cheng & Yoshizawa, 2019), the latter  
49  
50  
51 83 of which has normal genital structures, were also examined for comparison. All samples  
52  
53  
54 84 were subjected to  $\mu$ CT examination, and voucher specimens were stored in the  
55  
56  
57 85 Hokkaido University Insect Collection. Samples were fixed either with hot water, FAA  
58  
59  
60 86 solution (formalin:alcohol:acetic acid = 6:16:1), or 80% ethanol and then preserved in  
61  
62  
63  
64  
65

1 87 80% ethanol. Dehydration was conducted in ascending order with 80–100% ethanol  
2  
3 88 before drying them at the critical point (EM CPD300, Leica, Wetzlar, Germany) to  
4  
5  
6 89 remove water without serious organ shrinkage. Samples were then scanned by  
7  
8  
9 90 synchrotron  $\mu$ CT at the BL47XU (Uesugi et al., 2012) beamline of the Super Photon  
10  
11 91 ring-8 GeV (SPring-8; Hyogo, Japan) using a stable beam energy of 8 keV in  
12  
13  
14 92 absorption-contrast mode. The tomography system consists of a full-field X-ray  
15  
16  
17 93 microscope with Fresnel zone plate optics (Uesugi et al., 2017). We used semiautomatic  
18  
19  
20 94 segmentation algorithms based on grey-value differences in ITK-SNAP software  
21  
22  
23 95 (Yushkevich et al., 2006) to obtain 3D representations of the terminalia of all three  
24  
25  
26 96 species.

27  
28 97

## 30 98 **Results**

31  
32  
33 99 We first describe the muscles associated with male and female terminalia of *Neotrogla*  
34  
35  
36 100 *curvata*. We grouped the muscles according to their origin as follows: muscles of the  
37  
38  
39 101 epiproct [ep]; paraproct [pa]; subgenital plate [sg]; dorsal valve [do]; external valve  
40  
41  
42 102 [ex]; spermapore plate/gynosome or the membrane surrounding it [sp/gy]; hypandrium  
43  
44  
45 103 [hy]; and phallosome [ph].

46  
47  
48  
49 104 Abbreviations: O – origin; I – insertion; and F – assumed function based on  
50  
51  
52 105 morphological conditions.

53  
54  
55  
56 106 **epX01** (male/female) (Figs. 2C, D and 8A: = 01 of Cheng & Yoshizawa, 2019); O:  
57  
58  
59 107 mid-dorsal site of clunium (segment IX); I: posterior end of the epiproct; and F: closure

1 108 and/or flipping of the epiproct.  
2  
3  
4  
5 109 **paX01** (male/female) (Figs. 2C, D and 8A: = 02 of Cheng & Yoshizawa, 2019); O:  
6  
7 110 anterolateral region of the clunium (segment X); I: anterodorsal end of the paraproct,  
8  
9 111 very close to the posterolateral margin of the epiproct; and F: involved in opening the  
10  
11 112 paraproct.  
12  
13  
14  
15  
16  
17 113 **paX02** (male/female) (Figs. 2C, D and 8A: = 02 of Cheng & Yoshizawa, 2019); O:  
18  
19 114 mediodorsal region of the clunium (segment X); I: anterodorsal end of the paraproct,  
20  
21 115 very close to the anterolateral corner of the epiproct; and F: involved in opening the  
22  
23 116 paraproct.  
24  
25  
26  
27  
28  
29 117 **paX03** (male/female) (Figs. 2C, D and 8A: = 03 of Cheng & Yoshizawa, 2019); O:  
30  
31 118 mediolateral region of the clunium (segment X); I: internal margin of the paraproct near  
32  
33 119 the anal opening; and F: involved in retracting the paraproct.  
34  
35  
36  
37  
38  
39 120 **paX04** (male/female) (Figs. 2C, D and 8A); O: mediolateral region of the clunium  
40  
41 121 (segment IX); I: anterolateral margin of the paraproct; and F: involved in retracting the  
42  
43 122 paraproct.  
44  
45  
46  
47  
48  
49 123 **dosp01** (female) (Figs. 2E, F and 8A: = 05 of Cheng & Yoshizawa, 2019); O: base of  
50  
51 124 the dorsal valve; I: on the membrane connected to the spermapore plate/gynosome, near  
52  
53 125 the posterior tip of the spermapore plate; and F: involved in restoring the position of  
54  
55 126 the gynosome (spermapore plate) and the dorsal valve.  
56  
57  
58  
59 127 **doex01** (female) (Figs. 2E, F and 8A); O: base of the dorsal valve; I: base of the external  
60  
61  
62  
63  
64  
65

1 128 valve; and F: involved in restoring the position of the dorsal valve and closure of the  
2  
3 129 external valve.  
4  
5  
6 130 **exsp01** (female) (Figs. 2E, F and 8A: = 06 of Cheng & Yoshizawa, 2019); O: base of  
7  
8 131 the external valve; I: on the membrane connected to the spermapore plate/gynosome,  
9  
10 132 near the posterior tip of the spermapore plate; and F: involved in restoring the position  
11  
12 133 of the gynosome (spermapore plate) and closure of the external valve.  
13  
14  
15 134 **exIX02** (female) (Figs. 2E, F and 8A: = 08 of Cheng & Yoshizawa, 2019); O:  
16  
17 135 anterolateral margin of the clunium; I: base of the external valve, near the middle of the  
18  
19 136 junction with the clunium; and F: involved in opening the external valve.  
20  
21  
22 137 **exVIII01** (female) (Figs. 2E, F and 8A); O: medioventral region of sternum VIII; I:  
23  
24 138 base of the external valve; and F: involved in closure of the external valve.  
25  
26  
27 139 **spIX01** (female) (Figs. 2G, H and 8A); O: mediolateral region of the clunium; I: on the  
28  
29 140 spermapore membrane; and F: involved in restoring the gynosomal spiny membrane  
30  
31 141 (*Neotroglia*) or the position of the spermapore plate (other Psocodea).  
32  
33  
34 142 **spIX02** (female) (Figs. 2G, H and 8A); O: mediolateral region of the clunium; I: on  
35  
36 143 the spermapore membrane; and F: involved in restoring the gynosomal spiny  
37  
38 144 membrane (*Neotroglia*) or the position of the spermapore plate (other Psocodea).  
39  
40  
41 145 **gyIX01** (female) (Figs. 2G, H and 8A); O: gynosome membrane very close to dorsal  
42  
43 146 valves (=ventral membrane of segment IX); I: anterior end of the basal shaft; and F:  
44  
45 147 protractors of the gynosome.  
46  
47  
48 148 **gy-01** (female) (Figs. 2G, H and 8A); O: an internal organ (specific insertion site not  
49  
50 149 detected); I: anterior end of the basal shaft; and F: retractors of the gynosome.  
51  
52  
53  
54  
55  
56  
57  
58  
59  
60  
61  
62  
63  
64  
65



1 150 **papa01** (male) (Figs. 5C, D and 8B); O: internal margin of the paraproct near the anal  
2  
3 151 opening; I: anterolateral margin of the paraproct; and F: involved in opening the anus.

4  
5  
6 152 **pahy01** (male) (Figs. 3F, 5C, D and 8B: = 04 of Cheng & Yoshizawa, 2019); O:  
7  
8 153 anteroventral end of the paraproct; I: anterolateral region of the hypandrium (segment  
9  
10 154 IX); and F: involved in indirectly opening the hypandrium and retracting the male  
11  
12 155 paraproct (holding the female dorsal valve during copulation: see below).

13  
14  
15  
16  
17 156 **hyVIII01** (male) (Figs. 3F, 5E, F and 8B: = 05 of Cheng & Yoshizawa, 2019); O:  
18  
19 157 posterolateral region of segment VIII; I: mediolateral margin of the hypandrium; and F:  
20  
21 158 involved in restoring the hypandrium.

22  
23  
24  
25 159 **phIX01** (male) (Figs. 3F-I, 5G, H and 8B: = 07 of Cheng & Yoshizawa, 2019); O: U-  
26  
27 160 shaped end of the sclerite of the phallosome; I: anterolateral region of the hypandrium  
28  
29 161 (segment IX); and F: involved in opening the hypandrium/protrusion of the phallosome.

30  
31  
32  
33 162 **phIX02** (male) (Figs. 3F-I, 5G, H and 8B: = 08 of Cheng & Yoshizawa, 2019); O:  
34  
35 163 middle of the sclerite of the phallosome; I: anterolateral region of the hypandrium  
36  
37 164 (segment IX), phIX01, phIX02 and the sclerite of the phallosome present a triangle in  
38  
39 165 position; and F: involved in opening the hypandrium/retraction of the phallosome.

40  
41  
42  
43  
44 166 **phVIII01** (male) (Figs. 3F-I, 5G, H and 8B); O: posterolateral region of segment VIII;  
45  
46 167 I: posterior of the sclerite of the phallosome; and F: involved in protrusion of the  
47  
48 168 phallosome (holding the female dorsal valve during copulation: see below).

49  
50  
51  
52  
53 169

## 54 55 56 57 170 **Skeletal and muscle structures of female terminalia**

58  
59 171 Among the female terminal structures of *Neotroglia*, the morphology of the clunium and  
60  
61  
62  
63  
64  
65

1 172 the epiproct is not much different from those of the other females of Psocodea. In  
2  
3 173 contrast, the subgenital plate (posterior extension of the 8<sup>th</sup> sternum) is completely  
4  
5  
6 174 reduced in *Neotroglia*. A distinct difference was also detected in the paraproct between  
7  
8  
9 175 *Neotroglia* and other psocodeans, i.e., two concavities are present on the ventrolateral  
10  
11  
12 176 surface of the paraproct in *Neotroglia* (Fig. 1B). One group of muscles (epX01; Fig. 2C)  
13  
14  
15 177 is associated with the epiproct, and four groups of muscles (paX01-04; Fig. 2C) with  
16  
17  
18 178 the paraproct, all of which originate from the clunium. All of these muscles are  
19  
20  
21 179 homologous to those associated with the epiproct or paraproct of other psocodeans  
22  
23 180 (Cheng & Yoshizawa, 2022).

24  
25 181 The bases of the external valve of the gonapophyses are connected by a transverse  
26  
27  
28 182 sclerite (Fig. 3B). The dorsal valve of the gonapophyses is located posteromedially to  
29  
30  
31 183 the transverse sclerite of the external valves and forms an independent structure (Fig.  
32  
33  
34 184 1A). The dorsal valve is not truly a paired structure like the external valves. It is usually  
35  
36  
37 185 paired in Psocodea, but forms a single lobe-like structure with a posterior and lateral  
38  
39  
40 186 marginal ridge shaped like a chair with a central depression (Fig. 3A). Two groups of  
41  
42  
43 187 muscles (dosp01 and doex01; Fig. 2E) are connected to the dorsal valve. They are  
44  
45  
46 188 homologous with those associated with the dorsal valves of other psocodeans (Cheng  
47  
48 189 & Yoshizawa, 2022).

49  
50 190 The external valves form a pair of projections, together forming a crab claw-like  
51  
52  
53 191 structure, basally connected by a transverse sclerite. The transverse sclerite is laterally  
54  
55  
56 192 articulated with the clunium and anteriorly connected with sternum VIII (Fig. 1A, C).  
57  
58  
59 193 The external valves of both *Neotroglia* species show a similar morphology (Fig. 3C).  
60  
61  
62  
63  
64  
65

1 194 There are four groups of muscles (doex01, exsp01, exIX02, exVIII01; Fig. 2E)  
2  
3 195 connected to the external valve, and three groups of those muscles are homologous with  
4  
5  
6 196 those associated with the external valves of other psocodeans (Fig. 2E and 8A; Cheng  
7  
8  
9 197 & Yoshizawa, 2022). The exVIII01 muscle is unique to *Neotrogla*, and is observed in  
10  
11  
12 198 both species (Fig. 3C).

13  
14 199 The gynosome is composed of the apical sclerite, spiny membrane and basal shaft  
15  
16  
17 200 (Cheng et al., 2023). The gynosome is entirely placed anteriorly to the gonapophyses  
18  
19  
20 201 in the noncopulating state (Fig. 2A). During copulation, all parts other than the basal  
21  
22  
23 202 shaft protrude from the opening between the paraproct and gonapophyses (Fig. 1C, D).

24  
25 203 There are six groups of muscles (dosp01, exsp01, spIX01, spIX02, gyIX01, gy-01; Fig.  
26  
27  
28 204 2 E, G) connected to the gynosome, and four groups of those muscles are homologous  
29  
30  
31 205 with those associated with the spermapore plates of other psocodeans (Cheng &  
32  
33  
34 206 Yoshizawa, 2022). The gyIX01 (=M5 of Cheng et al., 2023) and gy-01 (= M6 of Cheng  
35  
36  
37 207 et al., 2023) muscles are unique to *Sensitibillini*.

38  
39 208

## 40 41 42 209 **Skeletal and muscle structures of male terminalia**

43  
44 210 Among the male terminal structures, no obvious specificity was detected for the  
45  
46  
47 211 clunium and epiproct. On the ventral side of each paraproct, a ridge is present, which  
48  
49  
50 212 is triangular in the lateral view (Fig. 4A, C). Hook-like protrusions are also observed  
51  
52  
53 213 on the paraproct of some other species of Psocodea but are generally located at the  
54  
55  
56 214 posterior end of the paraproct (Yoshizawa, 2005). One group of muscles is associated  
57  
58  
59 215 with the epiproct (epX01; Fig. 5C), and six groups of muscles with the paraproct

1 216 (paX01-04, papa01, pahy01; Fig. 5C). Among the latter, five groups of muscles  
2  
3 217 originate from the clunium, and one group of muscles originates from and inserts within  
4  
5  
6 218 the paraproct (Fig. 5C). Since the epiproct, paraproct and clunium are present in both  
7  
8  
9 219 sexes and have similar functions, five groups of muscles (epX01, paX01-04) can be  
10  
11 220 homologized between sexes (Fig. 5C and 8B; Cheng & Yoshizawa, 2022). The  
12  
13  
14 221 following two groups of muscles are unique to males.

16  
17 222 The hypandrium represents sternum IX and articulates laterally with the clunium.  
18  
19  
20 223 The hypandrium has no obvious protrusions in *Neotroglia* (Fig. 4A, C). One group of  
21  
22  
23 224 muscles is connected to the hypandrium (hyVIII01; Figs. 5E), which is homologous to  
24  
25  
26 225 that observed in *Trichadenotecnum* (Fig. 3D).

27  
28 226 The phallosome consists of two parts: a membranous pouch and a reversed U-  
29  
30  
31 227 shaped thin sclerite surrounding the posterodorsal margin of the entrance of the  
32  
33  
34 228 membranous pouch (Figs. 3F, G, 4E and 5A), which is only observed in *Neotroglia*  
35  
36  
37 229 species. The phallosome closely fits into the concavity formed by the hypandrium in a  
38  
39  
40 230 noncopulating state (Fig. 4E). During copulation, the sclerotized part of the phallosome  
41  
42  
43 231 is raised upwards, and its apex rests on the protrusions of the paraproctal ridges (Fig.  
44  
45  
46 232 4F). There are three groups of muscles (phIX01-02, phVIII01; Figs. 3F-I and 5G, H)  
47  
48  
49 233 connected to the phallosome. Among them, phIX01 and phIX02 were also observed in  
50  
51  
52 234 *Trichadenotecnum* (Fig. 3E).

### 53 235 **Male–female genital interaction**

54  
55  
56 236 In the copulating state, the male paraproct and epiproct are partly retracted inwardly.  
57  
58  
59 237 The ventral paraproctal ridges, which are separated in the noncopulated condition, are  
60  
61  
62  
63  
64  
65

1 238 closely associated during copulation, together forming a single projection (Fig. 4A-D).  
2  
3 239 The sclerite of the phallosome protrudes upwards, and its apex fits with the anterior  
4  
5  
6 240 margin of the male paraproctal projection (Fig. 4E, F). During copulation, these two  
7  
8  
9 241 male structures securely sandwich the female dorsal valve from both sides (Fig. 6B:  
10  
11  
12 242 blue arrow and Fig. 7: black dotted arrows).

13  
14 243 The male genital cavity formed by the hypandrium and phallosome is opened and  
15  
16  
17 244 exposed in the copulating condition (Fig. 4B, D). During copulation, the gynosome,  
18  
19  
20 245 with the exception of the basal shaft, extends into the male's genital cavity. The apical  
21  
22  
23 246 sclerite of the gynosome deeply penetrates the membranous pouch of the phallosome  
24  
25  
26 247 (Fig. 6B: red arrow and Fig. 7). The spiny membrane of the gynosome expands to form  
27  
28  
29 248 an internal anchor within the male genital cavity. The female epiproct and paraproct are  
30  
31  
32 249 slightly retracted inwards. The concave ventral surface of the female paraproct and the  
33  
34  
35 250 swollen gynosomal spiny area together anchor the male by sandwiching the  
36  
37  
38 251 hypandrium externally (paraproct) and internally (gynosomal spines) (Fig. 6B: white  
39  
40  
41 252 arrow and Fig. 7: red dotted arrows). The female external valves are opened and grasp  
42  
43  
44 253 the lateral sides of the hypandrium (Figs 1F, 6A and 7).

45 254

## 47 255 **Discussion**

### 50 256 **Copulation process and holding mechanisms**

52  
53 257 The present observation revealed that the following holding/locking systems are at  
54  
55  
56 258 work during copulation to stabilize the coupling condition: (1) the female dorsal valve  
57  
58  
59 259 is tightly sandwiched by the male paraproctal ridges and the tip of the phallosomal

1  
2  
3  
4  
5  
6  
7  
8  
9  
10  
11  
12  
13  
14  
15  
16  
17  
18  
19  
20  
21  
22  
23  
24  
25  
26  
27  
28  
29  
30  
31  
32  
33  
34  
35  
36  
37  
38  
39  
40  
41  
42  
43  
44  
45  
46  
47  
48  
49  
50  
51  
52  
53  
54  
55  
56  
57  
58  
59  
60  
61  
62  
63  
64  
65

1 260 sclerite; (2) the gynosomal spiny membrane anchors male internally by its inflation  
2  
3 261 within the male genital cavity; (3) the female paraproctal ventral concavities support  
4  
5  
6 262 the ventral surface of the male hypandrium, and the hypandrium is sandwiched by the  
7  
8  
9 263 female paraproct (ventrally) and the gynosomal spines (dorsally); and (4) the female  
10  
11  
12 264 external valves grasp the lateral side of the male abdominal tip.

13  
14 **265 Fixation of the female dorsal valve by the male**

15  
16  
17 266 During copulation, the female dorsal valve is almost fully inserted into the male and is  
18  
19  
20 267 tightly held by the male's structures (the paraproctal ridges and the tip of the  
21  
22  
23 268 phallosome sclerite; Figs 6B, red arrow and 7). In the copulating state, dosp01  
24  
25  
26 269 connected to the female dorsal valve is in a relaxed state (Fig. 2F). Therefore, it is  
27  
28  
29 270 assumed that this muscle is related to the re-storage of the dorsal valve at the end of  
30  
31  
32 271 copulation. No muscle related to the protrusion of the dorsal valve were found.

33  
34 272 Contractions of the male epiproctal and paraproctal muscles (epX01, paX01,  
35  
36 273 paX02, paX03, and pahy01) guide the male epiproct and paraproct to partly retract  
37  
38  
39 274 inwardly (Figs 4C, D and 5D). The paired male paraproctal ridges are tightly associated  
40  
41  
42 275 during copulation, together forming a single process, due to the contraction of paX03  
43  
44  
45 276 (Figs 4B, D and 5D). In the meantime, the contraction of the phVIII01 muscle pulls the  
46  
47  
48 277 phallosome upwards towards the paraproct (Figs 3I and 5H). The phIX01 muscle may  
49  
50  
51 278 also have the function of protruding the phallosome. The merged male paraproctal  
52  
53  
54 279 ridges buckle the ventral ridge of the female dorsal valve, and the other side of the  
55  
56  
57 280 female dorsal valve is supported by the tip of the phallosomal sclerite (Figs 6B, blue  
58  
59 281 arrow and 7, black dotted arrows). Furthermore, the contraction of the pahy01 muscle

1 282 provides strong power to securely make the paraproct hooking and pulling the female  
2  
3 283 dorsal valve inward. The phIX01 and phIX02 muscles may also produce additional  
4  
5  
6 284 power to move the apex of the phallosome inwards (i.e., pull the female dorsal valve  
7  
8  
9 285 inwards, Fig. 1E). This clearly shows that the male *Neotrogla* actively holds the female  
10  
11  
12 286 during copulation.

13  
14 287         Similar movement of the phallosome to hold and fix the female genital structure  
15  
16  
17 288 is also known in *Trichadenotecnum* (Psocomorpha: Psocidae: Cheng & Yoshizawa,  
18  
19  
20 289 2019). However, in the case of *Trichadenotecnum*, the male holds the subgenital plate,  
21  
22  
23 290 not the dorsal valve. In addition, the phIX01 and phIX02 muscles function to restore  
24  
25  
26 291 the phallosome, and the phVIII01 muscle is absent in *Trichadenotecnum*. Therefore,  
27  
28  
29 292 the female holding mechanism is apparently non-homologous between *Neotrogla* and  
30  
31 293 *Trichadenotecnum*.

32  
33  
34 294         At the end of the copulation, the paX01 and 02 muscles of the males are likely  
35  
36  
37 295 contracted to move the paraproct outwardly, and phIX01 is contracted to restore the  
38  
39  
40 296 phallosome. Both movements (active movements by the male) can function to release  
41  
42  
43 297 the grasp on the female dorsal valve.

#### 44 298 **Penetration of the gynosome and anchoring of the male**

45  
46  
47 299         To open the male genital cavity is very likely a prerequisite for the insertion of the  
48  
49  
50 300 gynosome by a female. This is probably caused by two factors: 1) retraction of the male  
51  
52  
53 301 paraprocts (see above), which are located above the genital chamber under  
54  
55  
56 302 noncopulating conditions, thus blocking the male genital opening, and 2) backwards  
57  
58  
59 303 movement of the posterior margin of the hypandrium. There is no muscle that causes  
60  
61  
62  
63  
64  
65

1 304 direct backwards movement of the posterior margin of the hypandrium. However, as  
2  
3 305 seen from Fig. 4B, the male terminalia are strongly compressed laterally during  
4  
5  
6 306 copulation, which is very likely to cause the indirect backwards movement of the  
7  
8  
9 307 posterior margin of the hypandrium (such as the mouth of a spring-loaded coin purse).  
10  
11 308 From the reconstructed 3D model of the copulating condition, two factors can be  
12  
13  
14 309 assumed to be associated with the lateral compression of the male terminalia: 1)  
15  
16  
17 310 contraction of the pahy01, phIX01 and 02 muscles causes the inward movement of the  
18  
19  
20 311 lateral side of the hypandrium (i.e., male active movement); 2) grasping by the female  
21  
22  
23 312 external valves causes compression force of the male terminalia (i.e., passive movement  
24  
25  
26 313 for the male: see below).

27  
28 314 The phIX01 and phIX02 muscles share the same origin on the hypandrium,  
29  
30  
31 315 together forming a triangular configuration with the sclerite of the phallosome (Fig. 3H,  
32  
33  
34 316 I). This state allows the hypandrium to move more effortlessly because the forces  
35  
36  
37 317 generated by the two muscles are in the same plane. If the insertion site of these two  
38  
39  
40 318 muscles on the hypandrium is not consistent, it is difficult to ensure that all the forces  
41  
42  
43 319 are on the same plane, which will easily lead to conflicting forces. A similar  
44  
45  
46 320 arrangement of the muscles has also been observed in the female external valves  
47  
48  
49 321 (exIV01 and exIV02) of other psocodeans, such as *Lepinotus* and Amphientomidae,  
50  
51  
52 322 which is also considered to cause effective movements of the valve (Cheng &  
53  
54  
55 323 Yoshizawa, 2022).

56 324 Regarding the muscles attached to the gynosome, gy-01 relaxes and gyIX01  
57  
58  
59 325 contracts in the copulating condition, and the status of these two muscles vice versa in  
60  
61  
62  
63  
64  
65



1 326 the non-copulating condition. Therefore, the contraction of gyIX01 apparently has a  
2  
3 327 function to extend the gynosome, and gy-01 works to restore the stuck gynosome to the  
4  
5  
6 328 resting position (Fig. 2G, H). Two stout muscles, spIX01 and spIX02, relax during  
7  
8  
9 329 copulation, thus restoring the gynosome membrane to its original shape and position  
10  
11 330 (Fig. 2G, H). The apical sclerite of the gynosome deeply penetrates the membranous  
12  
13  
14 331 pouch of the phallosome during copulation, from which the semen is transported to the  
15  
16  
17 332 female (Yoshizawa et al., 2014). The spiny membrane of the gynosome also enters the  
18  
19  
20 333 male genital cavity (Figs. 1C, D, 6B and 7). Because no muscle is involved in inflating  
21  
22  
23 334 the spiny membrane, the anchoring function of this specialized membrane is likely  
24  
25  
26 335 achieved by increased body pressure. See also the next section for the additional  
27  
28  
29 336 holding function of the gynosomal spines.

30  
31 337 At the end of copulation, reduction of the internal pressure can cause the deflation  
32  
33  
34 338 of the spiny membrane, and the contraction of the spIX01 and 02 muscles acts to restore  
35  
36  
37 339 the gynosomal spiny membrane. The gynosome is retracted by the contraction of the  
38  
39  
40 340 gy-01 muscle.

#### 41 42 341 **Ventral fixation of the hypandrium**

43  
44 342 The female paX01 and paX02 muscles are contracted during copulation, causing the  
45  
46  
47 343 paraproct to be slightly indented in the direction of the female epiproct (Fig. 2D). The  
48  
49  
50 344 female paX03 muscle retracts during copulation, directing the protrusions on the ventral  
51  
52  
53 345 surface of the female paraproct inward (Figs. 1D and 2D). By this movement, the  
54  
55  
56 346 ventrolateral paraproctal concavities form a continuous single circular concavity, which  
57  
58  
59 347 fits perfectly to the curve of the ventral margin of the hypandrium (Fig. 6B, white  
60  
61  
62  
63  
64  
65

1 348 arrow).

2  
3 349 The jointed female paraproctal cavities support the ventral surface of the male  
4  
5  
6 350 hypandrium externally during copulation, which sandwich the hypandrium together  
7  
8  
9 351 with the gynosomal spiny anchor within the male genital chamber (Figs. 6B, white  
10  
11  
12 352 arrow and 7). Therefore, it is apparent that the female actively holds the male during  
13  
14  
15 353 copulation by using the female paraproct and gynosome. Such close contact between  
16  
17 354 the female paraproct and the male hypandrium is not observed in *Trichadenotecnum*  
18  
19  
20 355 (Cheng & Yoshizawa, 2019).

21  
22  
23 356 At the end of copulation, paX01 and 02 are probably contracted to release the  
24  
25  
26 357 ventral paraproctal support of the male hypandrium.

### 27 28 358 **Grasping the male abdomen by the female external valves**

29  
30  
31 359 The exIX02 muscle is contracted during copulation and thus is associated with the  
32  
33  
34 360 active opening of the female external valve at the beginning of copulation (Fig. 1C, F).

35  
36 361 The female external valves grasp the lateral surface of the male hypandrium with  
37  
38  
39 362 the contraction of the stout doex01 and exVIII01 muscles (Figs. 2E, F, 6A and 7). As  
40  
41  
42 363 also mentioned above, this probably comprises two functions: opening the male genital  
43  
44  
45 364 cavity at the beginning of copulation and holding the male during copulation, both of  
46  
47  
48 365 which are active movements of the female.

49  
50 366 At the end of copulation, exIX02 is probably contracted to open the external valves  
51  
52  
53 367 to release the grasp on the male.

54  
55  
56 368 The functions of the muscles related to the external valve (opening/closing the  
57  
58  
59 369 external valves) are also common in *Trichadenotecnum*. However, the external valve  
60  
61  
62  
63  
64  
65

1 370 of *Trichadenotecnum* does not have a function to grasp the male, and its closure muscles  
2  
3 371 hold the female subgenital plate, possibly to resist coercive mating by males (Cheng &  
4  
5  
6 372 Yoshizawa, 2019).  
7

8  
9 **373 Sexual selection**

10  
11 374 In animals with conventional sex roles, females usually gain fewer fitness benefits from  
12  
13  
14 375 multiple matings, and thus, males more actively seek mating opportunities (Trivers,  
15  
16  
17 376 1972). Accordingly, male animals sometimes develop elaborate genital structures for  
18  
19  
20 377 coercive copulation with unwilling mates (Arnqvist & Rowe, 2002; Lange et al., 2013).  
21  
22  
23 378 As counteradaptations, two types of traits are known to occur in female genitals:  
24  
25  
26 379 “resistance” traits that decrease the male fitness component (e.g., efficiency of mate  
27  
28  
29 380 holding) and “tolerance” traits that mitigate the costs of mating without affecting male  
30  
31  
32 381 mating success (Reinhardt et al., 2014). In *Neotrogla*, males give nutritious seminal  
33  
34  
35 382 gifts to females during copulation, which last up to 72 hours, and females mate multiply,  
36  
37  
38 383 as is evident from the occurrence of multiple seminal capsules in the spermatheca  
39  
40  
41 384 (Yoshizawa et al., 2014, 2018a). In addition, female *Neotrogla* possess twin  
42  
43  
44 385 insemination slots with switching valves to receive double seminal gifts at the same  
45  
46  
47 386 time (Yoshizawa et al., 2018a; Kamimura et al., 2021). Therefore, it has been assumed  
48  
49  
50 387 in previous studies that female *Neotrogla* gain more net benefits from multiple  
51  
52  
53 388 copulations than males and that females actively control copulatory processes by using  
54  
55  
56 389 the unique intromittent organ (coupling-role reversal: Yoshizawa et al., 2014, 2019).

57  
58  
59 390 Our present study confirmed this view by showing that the multiple female organs  
60  
61  
62 391 actively (and probably partly coercively) hold the male mate: this is achieved by  
63  
64  
65

1 392 anchoring within the male genital chamber using the gynosomal spines and external  
2  
3 393 grasping using the female paraproct and the external valves. However, at the same time,  
4  
5  
6 394 the 3D models also revealed that autonomous movements of male genital muscles are  
7  
8  
9 395 necessary for the initiation of the copulatory processes and that male *Neotrogla* actively  
10  
11  
12 396 hold the female mate during copulation.

13  
14 397 The male paraproctal ridges and the tip of the phallosomal sclerite are tightly  
15  
16  
17 398 associated even in the non-copulating condition in both *N. curvata* and *N. brasiliensis*  
18  
19  
20 399 (Figs. 4A, C and 6C, D) and, without active upwards movement of the paraproct  
21  
22  
23 400 (contraction of the paX01 and 02 muscles) of the male and downwards movement of  
24  
25  
26 401 the phallosome (contraction of the phIX02 muscle), the female cannot insert the dorsal  
27  
28 402 valve into the genital cavity. To open the genital cavity is the most important  
29  
30  
31 403 prerequisite for gynosomal insertion, and although its opening may partly be achieved  
32  
33  
34 404 by the female's active movements (i.e., grasping of the terminalia using the external  
35  
36  
37 405 valve), some male muscles (pahy01, phIX01 and phIX02) seem to be related to the  
38  
39 406 autonomous opening of the genital cavity. These male structures may also act to resist  
40  
41  
42 407 coercive copulation by females.

43  
44  
45 408 In addition, the male securely fixes the female dorsal valve during copulation using  
46  
47  
48 409 the male paraproctal ridges and the phallosomal sclerite. The well-developed male  
49  
50  
51 410 muscles related to this fixation function, including some uniquely developed in  
52  
53 411 *Neotrogla*, strongly suggest that the secure holding of the mate during copulation is  
54  
55  
56 412 also crucial for the male.

57  
58  
59 413 For some animals with conventional sex roles, mismatching in genital coupling is  
60  
61  
62  
63  
64  
65

1 414 known to result in leakage of seminal fluid, which can cause the female and male bodies  
2  
3 415 to stick together and thus reduce the rate of sperm transfer (Kamimura & Mistumoto,  
4  
5  
6 416 2012; Tanaka et al., 2018; Polak & McEvey, 2022), or increasing the wounding  
7  
8  
9 417 probability of the female genitals (Sota & Kubota, 1998; Kamimura, 2012; Masly &  
10  
11 418 Kamimura, 2014). In many of those cases, the females develop specific structures (such  
12  
13  
14 419 as membranous pockets) that accommodate the wound-inflicting structures of the male  
15  
16  
17 420 genitalia and thus mitigate the copulatory costs (Sota & Kubota, 1998; Kamimura,  
18  
19  
20 421 2012). Interestingly, male *Neotroglia* possess species-specific pockets on the walls of  
21  
22 422 the genital chamber to receive gynosomal spines, although no copulatory wounds have  
23  
24  
25 423 been detected there (Yoshizawa et al., 2014). Given that the copulatory mechanism of  
26  
27  
28 424 *Neotroglia* is complicated, seminal fluid passed to the female is voluminous and  
29  
30  
31 425 possibly reactive (Yoshizawa et al., 2014). Considering that the females' anchoring  
32  
33  
34 426 power is very strong (an artificial trial to separate a coupled specimen led to separation  
35  
36 427 of the male abdomen from the thorax without breaking the genital coupling: Yoshizawa  
37  
38  
39 428 et al., 2014), a precisely connected genital complex and step-by-step releases of each  
40  
41  
42 429 holding mechanism achieved by the cooperation of both sexes are probably beneficial  
43  
44  
45 430 for both males and females. Such concordance of the interests between the sexes may  
46  
47  
48 431 have prompted the evolution of "tolerance" traits in male *Neotroglia*, as in a completely  
49  
50  
51 432 sex-role reversed mating scenario.

52  
53 433

54  
55  
56 434 **Conclusion**

57  
58 435 Inverted genital couplings of *Neotroglia* provide an extremely rare opportunity to test  
59  
60  
61  
62  
63  
64  
65

1 436 hypotheses on the evolution of genital structures (House & Simmons, 2006; Simmons,  
2  
3 437 2014; Michels et al., 2015) under the reversed direction of sexual selection. We found  
4  
5  
6 438 evidence of the complicated coexistence of genital structures, suggesting male  
7  
8  
9 439 resistance, female coercion, and cooperation between the sexes. The absence of harmful  
10  
11  
12 440 structures that inflict wounds on the opposite sex in both males and females is notable.  
13  
14  
15 441 The coevolution between the male and female genital structures in *Neotroglia* may  
16  
17  
18 442 provide a new example for the evolution of tolerance traits, a newly proposed idea  
19  
20  
21 443 concerning genital evolution (Michels et al., 2015).

22  
23 444 For further understanding of the sexual selection and evolution of novelties,  
24  
25  
26 445 detailed information of the courtship behaviour of *Neotroglia* and its relatives is key but  
27  
28  
29 446 is very poorly understood to date. Accumulation of basic behavioural information is  
30  
31  
32 447 highly desired for a more accurate and detailed understanding of the evolution of the  
33  
34  
35 448 gynosome in *Neotroglia*.

36  
37 449

## 40 450 **Acknowledgement**

41  
42  
43 451 We thank Kentaro Uesugi for support with the  $\mu$ CT imaging. Research at Spring-  
44  
45  
46 452 8 was approved through project numbers 2016A1269 (leader: Ryuichiro Machida),  
47  
48  
49 453 2017B1712 and 2018B1725 (Naoki Ogawa). This work was supported by Japan  
50  
51  
52 454 Society for the Promotion of Science, grant numbers 20J2088301 to ZC and 15H04409  
53  
54  
55 455 and 19H03278 to KY. RLF thanks the Conselho Nacional de Desenvolvimento  
56  
57  
58 456 Científico e Tecnológico (CNPq grant n. 308334/2018-3).

1 457

2  
3  
4  
5 458 **Declarations**

6  
7  
8 459 **Conflict of Interest** The authors declare no conflict of interests

9  
10  
11 460

12  
13  
14 461 **References**

15  
16 462 Arnqvist G, Rowe L (2002) Correlated evolution of male and female morphologies in  
17 water striders. *Evolution* 56:936–947. [https://doi.org/10.1111/j.0014-](https://doi.org/10.1111/j.0014-3820.2002.tb01406.x)  
18  
19 463  
20  
21 464 3820.2002.tb01406.x

22  
23  
24 465 Cheng Z, Yoshizawa K (2019) Functional morphology of Trichadenotecnum male and  
25 female genitalia analyzed using  $\mu$ CT (Insecta: Psocodea: Psocomorpha). *J Morph* 280:  
26 466 555-567. <https://doi.org/10.1002/jmor.20965>  
27  
28 467

29  
30  
31 468 Cheng Z, Yoshizawa K (2022) Exploration of the homology among the muscles  
32 associated with the female genitalia of the three suborders of Psocodea  
33 469 associated with the female genitalia of the three suborders of Psocodea  
34 (Insecta). *Arthropod Str Dev* 66:101141. <https://doi.org/10.1016/j.asd.2022.101141>  
35  
36 470

37  
38  
39 471 Cheng Z, Kamimura Y, Ferreira RL, Lienhard C, Yoshizawa K (2023) Acquisition of  
40 472 novel muscles enabled protruding and retracting mechanisms of female penis in sex-  
41 role reversed cave insects. *Roy Soc Open Sci.* 10:220471. [10.1098/rsos.220471](https://doi.org/10.1098/rsos.220471)  
42  
43 473

44  
45  
46  
47 474 Gwynne DT (2008) Sexual conflict over nuptial gifts in insects. *Ann Rev Entomol* 53:  
48 475 83-101. [10.1146/annurev.ento.53.103106.093423](https://doi.org/10.1146/annurev.ento.53.103106.093423)

49  
50  
51  
52 476 House CM, Simmons LW (2006) Offensive and defensive sperm competition roles in  
53 the dung beetle *Onthophagus taurus* (Coleoptera: Scarabaeidae). *Behav Ecol Sociobiol*  
54 477 60:131-136. <https://www.jstor.org/stable/25063796>  
55  
56 478

57  
58  
59  
60 479 Kamimura Y (2012) Correlated evolutionary changes in *Drosophila* female genitalia  
61  
62  
63  
64  
65

1 480 reduce the possible infection risk caused by male copulatory wounding. Behav Ecol  
2 Sociobiol 66:1107-1114. 10.1007/s00265-012-1361-0  
3  
4  
5  
6 482 Kamimura Y, Mitsumoto H (2012) Lock- and- key structural isolation between sibling  
7  
8 483 *Drosophila* species. Entomol Sci 15:197-201. <https://doi.org/10.1111/j.1479->  
9  
10 484 8298.2011.00490.x  
11  
12  
13 485 Kamimura Y, Yoshizawa K, Lienhard C, Ferreira RL, Abe J (2021) Evolution of nuptial  
14  
15 486 gifts and its coevolutionary dynamics with male-like persistence traits of females for  
16  
17 487 multiple mating. BMC Ecol Evol 21:164. <https://doi.org/10.1186/s12862-021-01901-x>  
18  
19  
20  
21 488 Klier E (1956) Zur Konstruktionsmorphologie des männlichen Geschlechtsapparates  
22  
23 489 der Psocopteren. Zool Jahr (Anat.) 75:207–286.  
24  
25  
26 490 Lange R, Reinhardt K, Michiels NK, Anthes N (2013) Functions, diversity, and  
27  
28 491 evolution of traumatic mating. Biol Rev 88:585–601. 10.1111/brv.12018  
29  
30  
31  
32 492 Lewis S, South A (2012) The evolution of animal nuptial gifts. In *Advances in the Study*  
33  
34 493 *of Behavior* (Vol. 44, pp. 53-97). Academic Press. 10.1016/B978-0-12-394288-  
35  
36 494 3.00002-2  
37  
38  
39 495 Lienhard C (1998) Psocoptères euro-méditerranéens. Faune France 83:1-517.  
40  
41  
42  
43 496 Lienhard C (2007) Description of a new African genus and a new tribe of  
44  
45 497 Speleketorinae (Psocodea: 'Psocoptera': Prionoglarididae). Rev suisse Zool 114:441-  
46  
47 498 469. 10.5962/bhl.part.80399  
48  
49  
50  
51 499 Lienhard C, Carmo TOD, Ferreira RL (2010) A new genus of Sensitibillini from  
52  
53 500 Brazilian caves (Psocodea: 'Psocoptera': Prionoglarididae) Rev Suisse Zool 117:611-635.  
54  
55 501 10.5962/bhl.part.117600  
56  
57  
58 502 Lienhard C, Ferreira RL (2013) A new species of *Neotroglia* from Brazilian caves  
59  
60 503 (Psocodea:'Psocoptera': Prionoglarididae). Rev Suisse Zool 120:3-12.  
61  
62  
63  
64  
65



1 504 Masly JP, Kamimura Y (2014) Asymmetric mismatch in strain-specific genital  
2 morphology causes increased harm to *Drosophila* females. *Evolution* 68:2401-2411.  
3  
4 506 10.1111/evo.12436  
5  
6  
7  
8 507 Michels J, Gorb SN, Reinhardt K (2015) Reduction of female copulatory damage by  
9 resilin represents evidence for tolerance in sexual conflict. *J Roy Soc*  
10 508 *Interface* 12:20141107. 10.1098/rsif.2014.1107  
11  
12 509  
13  
14  
15 510 Polak M, McEvey SF (2022) Refutation of traumatic insemination in the *Drosophila*  
16 *bipunctinata* species complex. *Biol Lett* 18:20210625.  
17 511 <https://doi.org/10.1098/rsbl.2021.0625>  
18  
19 512  
20  
21  
22  
23 513 Simmons LW (2014). Sexual selection and genital evolution. *Austral Entomol* 53:1-  
24  
25 514 17. <https://doi.org/10.1111/aen.12053>  
26  
27  
28  
29 515 Sota T, Kubota K (1998) Genital lock- and- key as a selective agent against  
30 hybridization. *Evolution* 52:1507-1513. 10.1111/j.1558-5646.1998.tb02033.x  
31 516  
32  
33  
34  
35 517 Tanaka KM, Kamimura Y, Takahashi A (2018) Mechanical incompatibility caused by  
36 modifications of multiple male genital structures using genomic introgression in  
37 518 *Drosophila*. *Evolution* 72:2406-2418. 10.1111/evo.13592  
38  
39 519  
40  
41  
42  
43 520 Trivers RL (1972). Parental investment and sexual selection. In *Sexual Selection and*  
44 521 *the Descent of Man, 1871–1971*. Aldine Publishing.  
45  
46  
47  
48  
49 522 Uesugi K, Hoshino M, Takeuchi A, Suzuki Y, Yagi N (2012) Development of fast and  
50 523 high throughput tomography using CMOS image detector at SPring-8. *Dev X-Ray*  
51  
52 524 Tomography VIII 8506:85060I. 10.1117/12.929575  
53  
54  
55  
56  
57  
58 525 Uesugi K, Hoshino M, Takeuchi A (2017) Introducing high efficiency image detector  
59  
60  
61  
62  
63  
64  
65

1 526 to X-ray imaging tomography. J Phys Conference Series 849:012051. 10.1088/1742-  
2  
3 527 6596/849/1/012051  
4  
5  
6  
7 528 Yoshizawa K (2001) A systematic revision of Japanese *Trichadenotecnum* Enderlein  
8  
9 529 (Psocodea:'Psocoptera': Psocidae: Ptyctini), with redefinition and subdivision of the  
10  
11 530 genus. Invertebr Syst 15:159–204. 10.1071/IT00013  
12  
13  
14 531 Yoshizawa K (2005) Morphology of Psocomorpha (Psocodea:' Psocoptera'). Insecta  
15  
16 532 Matsumurana NS 62:1–44.  
17  
18  
19  
20 533 Yoshizawa K, Ferreira RL, Kamimura Y, Lienhard C (2014) Female penis, male vagina,  
21  
22 534 and their correlated evolution in a cave insect. Curr Biol 24:1006-1010.  
23  
24 535 <https://doi.org/10.1016/j.cub.2014.03.022>  
25  
26  
27 536 Yoshizawa K, Kamimura Y, Lienhard C, Ferreira RL, Blanke A (2018a) A biological  
28  
29 537 switching valve evolved in the female of a sex-role reversed cave insect to receive  
30  
31 538 multiple seminal packages. eLife 7:e39563. 10.7554/eLife.39563.  
32  
33  
34  
35 539 Yoshizawa K, Ferreira RL, Yao I, Lienhard C, Kamimura Y (2018b) Independent  
36  
37 540 origins of female penis and its coevolution with male vagina in cave insects (Psocodea:  
38  
39 541 Prionoglarididae). Biol Lett 14:20180533. <https://doi.org/10.1098/rsbl.2018.0533>  
40  
41  
42 542 Yoshizawa K, Ferreira RL, Lienhard C, Kamimura Y (2019) Why did a female penis  
43  
44 543 evolve in a small group of cave insects?. BioEssays 41:1900005.  
45  
46 544 10.1002/bies.201900005  
47  
48  
49  
50  
51 545 Yushkevich PA, Piven J, Hazlett HC, Smith RG, Ho S, Gee JC, Gerig G (2006) User-  
52  
53 546 guided 3D active contour segmentation of anatomical structures: significantly  
54  
55 547 improved efficiency and reliability. Neuroimage 31:1116-1128.  
56  
57 548 <https://doi.org/10.1016/j.neuroimage.2006.01.015>  
58  
59  
60  
61  
62  
63  
64  
65

1 549 **Figure Legends**

2  
3 550 **Fig. 1.** 3D reconstruction of the female terminalia of *Neotroglia curvata*; (for E-G left:  
4  
5  
6 551 noncopulating state; right: copulating state): (A) ventral view, noncopulating state; (B)  
7  
8 552 posterior view, noncopulating state; (C) ventral view, copulating state; (D) posterior  
9  
10 553 view, copulating state; (E) lateral view (highlighting dorsal valve); (F) lateral view  
11  
12 554 (highlighting the external valve); (G) lateral view (highlighting the gynosome).  
13  
14  
15  
16  
17 555 Abbreviations: ep = epiproct; pa = paraproct; cl = clunium; st = sternum; gy =  
18  
19 556 gynosome; do = dorsal valve; ex = external valve.  
20  
21

22 557 **Fig. 2.** 3D reconstruction of the female terminalia of *Neotroglia curvata*, internal view;  
23  
24 558 noncopulating state (A, C, E and G ); copulating state (B, D, F, and H); highlighting  
25  
26 559 different structures and associated muscles (C-H): (1) epX01; (2) paX01; (3) paX02;  
27  
28 560 (4) paX03; (5) paX04; (6) dosp01; (7) doex01; (8) exsp01; (9) exIX02; (10) exVIII01;  
29  
30 561 (11) spIX01; (12) spIX02; (13) gygy01; (14) gy-01. See Fig. 1 for abbreviations.  
31  
32  
33  
34  
35

36 562

37  
38  
39  
40 563 **Fig. 3.** 3D reconstruction of the terminalia in the noncopulating state (A-H) and  
41  
42 564 copulating state (I), highlighting different structures and associated muscles: female  
43  
44 565 *Neotroglia curvata* (A,B); female *N. brasiliensis* (C); male *Trichadenotecnum*  
45  
46 566 *pseudomedium* (D,E); male *N. brasiliensis* (F,G); male *N. curvata* (H,I). (A-C) Ventral  
47  
48 567 view; (D-F) internal view; (G-I) lateral view. Abbreviations: ep = epiproct; pa =  
49  
50 568 paraproct; hy = hypandrium; cl = clunium; ph = phallosome.  
51  
52  
53  
54  
55  
56

57 569

58  
59 570 **Fig. 4.** 3D reconstruction of the male terminalia of *Neotroglia curvata*, noncopulating  
60  
61  
62  
63  
64  
65

1 571 state (A, C and E); copulating state (B, D and F): (A, B) posterior view; (C, D) lateral  
2  
3 572 view; (E, F) lateral view (highlighting the phallosome). Abbreviations: sg = segment  
4  
5  
6 573 VIII; m= membrane; for others, see Fig. 3.

7  
8  
9 574 **Fig. 5.** 3D reconstruction of the male terminalia of *Neotroglia curvata*, internal view;  
10  
11 575 noncopulating state (A, C, E and G); copulating state (B, D, F and H), highlighting  
12  
13 576 different structures and associated muscles (D-H): (1) epX01; (2) paX01; (3) paX02;  
14  
15 577 (4) paX03; (5) paX04; (6) pahy01; (7) papa01; (8) hyVIII01; (9) phIX01; (10) phIX02;  
16  
17 578 (11) phVIII01. Abbreviations: te = tergum; m= membrane; for others, see Fig. 3.

18  
19  
20 579 **Fig. 6.** *Neotroglia curvata*, 3D reconstruction of terminalia of the copulating pair, lateral  
21  
22 580 view (A,B); *N. brasiliensis*, 3D reconstruction of terminalia of the male in the  
23  
24 581 noncopulating state (C,D). (B) highlighting the gynosome, phallosome, paraproct (m)  
25  
26 582 and epiproct (m); (C) posterior view; (D) lateral view, highlighting the phallosome and  
27  
28 583 paraproct (m). See Figs. 1 and 3 for abbreviations.

29  
30  
31 584 **Fig. 7.** Schematic drawing of the male and female genitalia of *Neotroglia curvata*  
32  
33 585 in copulated condition. Gray indicates male structures, and orange indicates female  
34  
35 586 ones. Black arrows indicate holding system by male, and red arrows indicate that by  
36  
37 587 female.

38  
39  
40 588 **Fig.8.** *Neotroglia curvata* in an uncopulated state, putative groundplan configuration of  
41  
42 589 the terminalia (internal view), schematic (based on the 3D reconstruction of the *N.*  
43  
44 590 *curvata*). (a) female; (b) male. Lines indicate muscles. Except for muscle paX04, all  
45  
46 591 dotted lines indicate the muscles attached to the gynosome membrane. (1) epX01; (2)  
47  
48 592 paX01; (3) paX02; (4) paX03; (5) paX04; (6) dosp01; (7) doex01; (8) exsp01; (9)

1 593 exIX02; (10) exVIII01; (11) spIX01; (12) spIX02; (13) gygy01; (14) gy-01; (15)  
2  
3 594 pahy01; (16) papa01; (17) hyVIII01; (18) phIX01; (19) phIX02; (20) phVIII01. See  
4  
5  
6 595 Figs. 1 and 3 for abbreviations.  
7  
8  
9 596  
10  
11  
12  
13  
14  
15  
16  
17  
18  
19  
20  
21  
22  
23  
24  
25  
26  
27  
28  
29  
30  
31  
32  
33  
34  
35  
36  
37  
38  
39  
40  
41  
42  
43  
44  
45  
46  
47  
48  
49  
50  
51  
52  
53  
54  
55  
56  
57  
58  
59  
60  
61  
62  
63  
64  
65

Figure 1

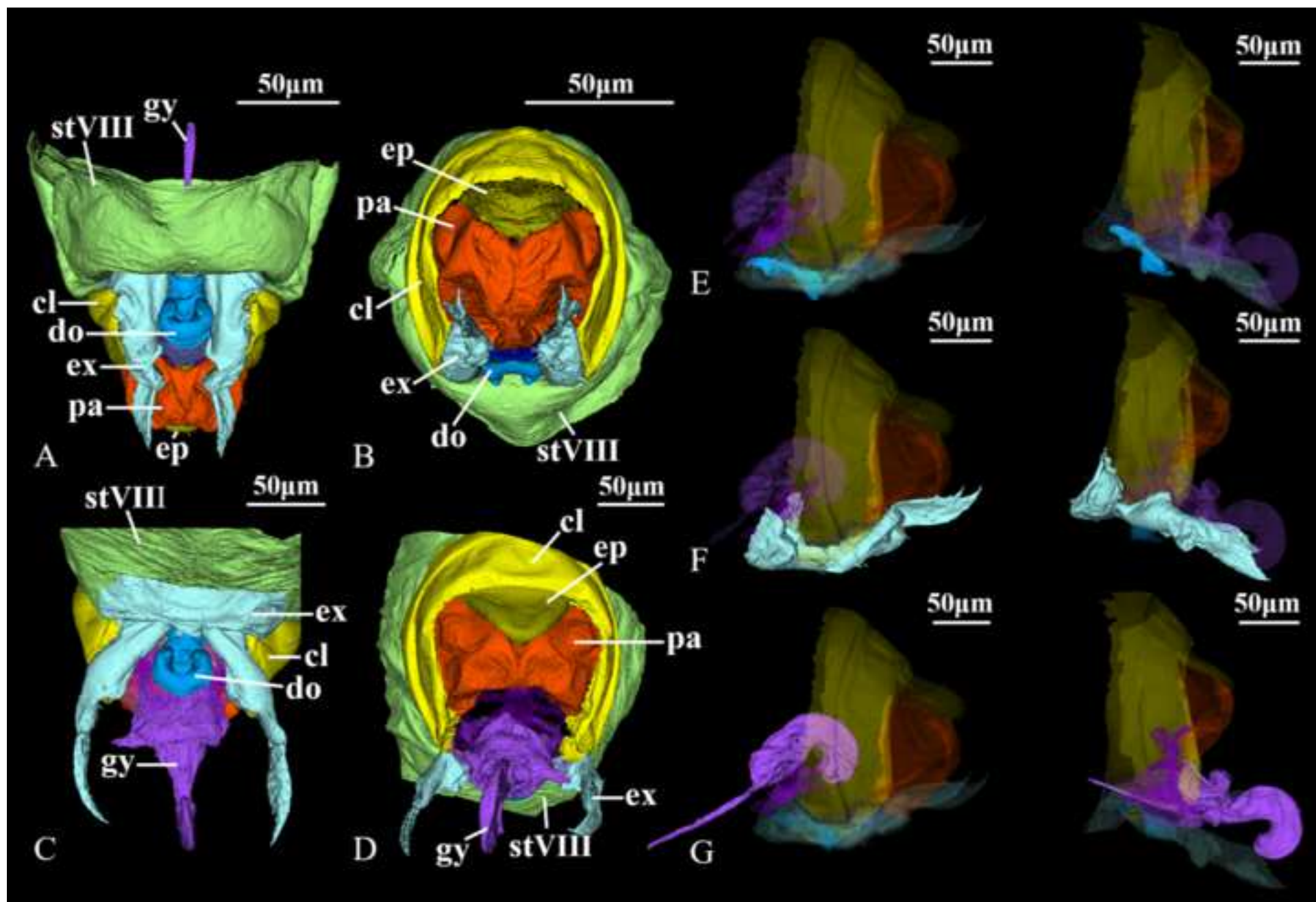


Figure 2

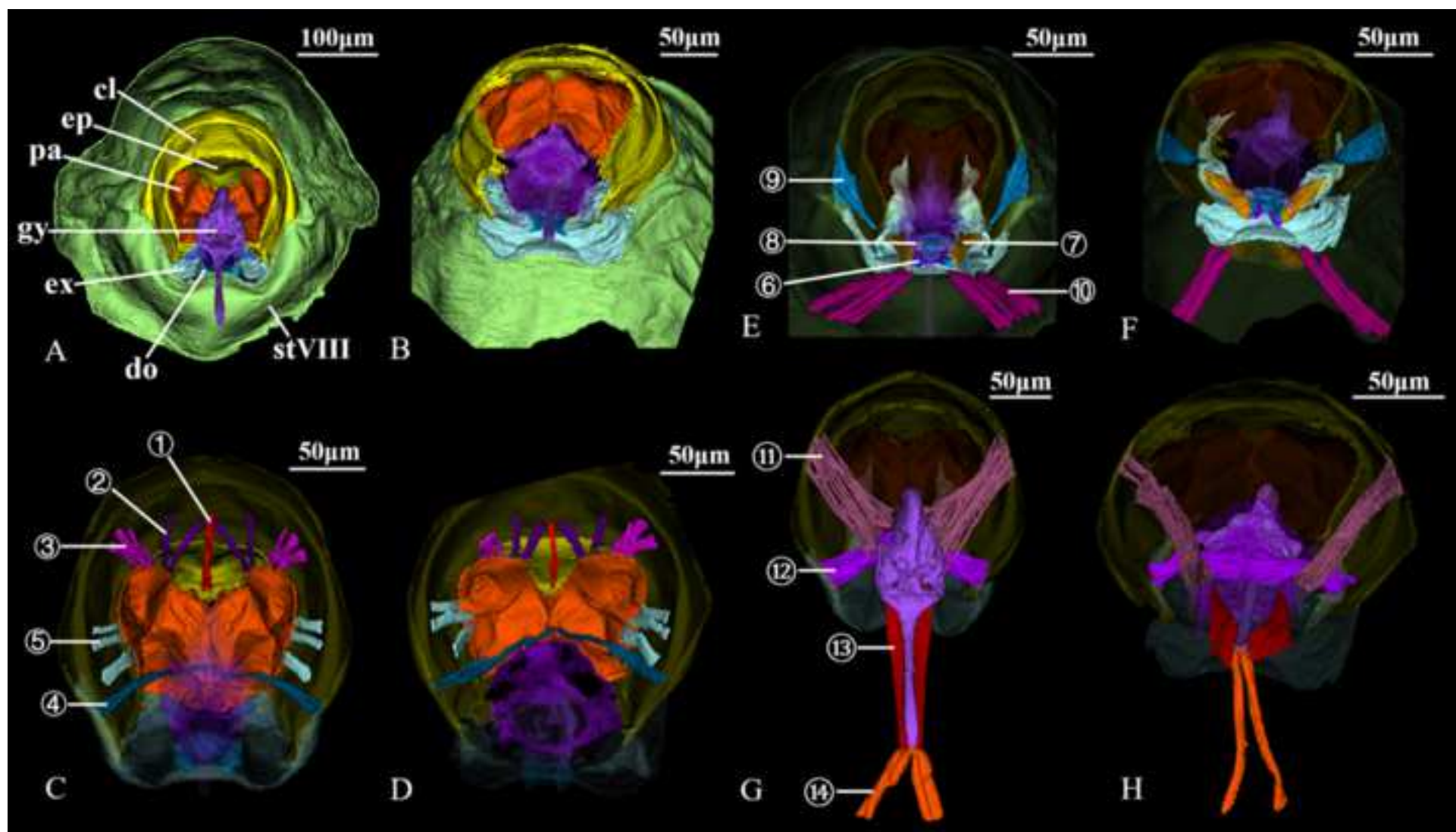


Figure 3

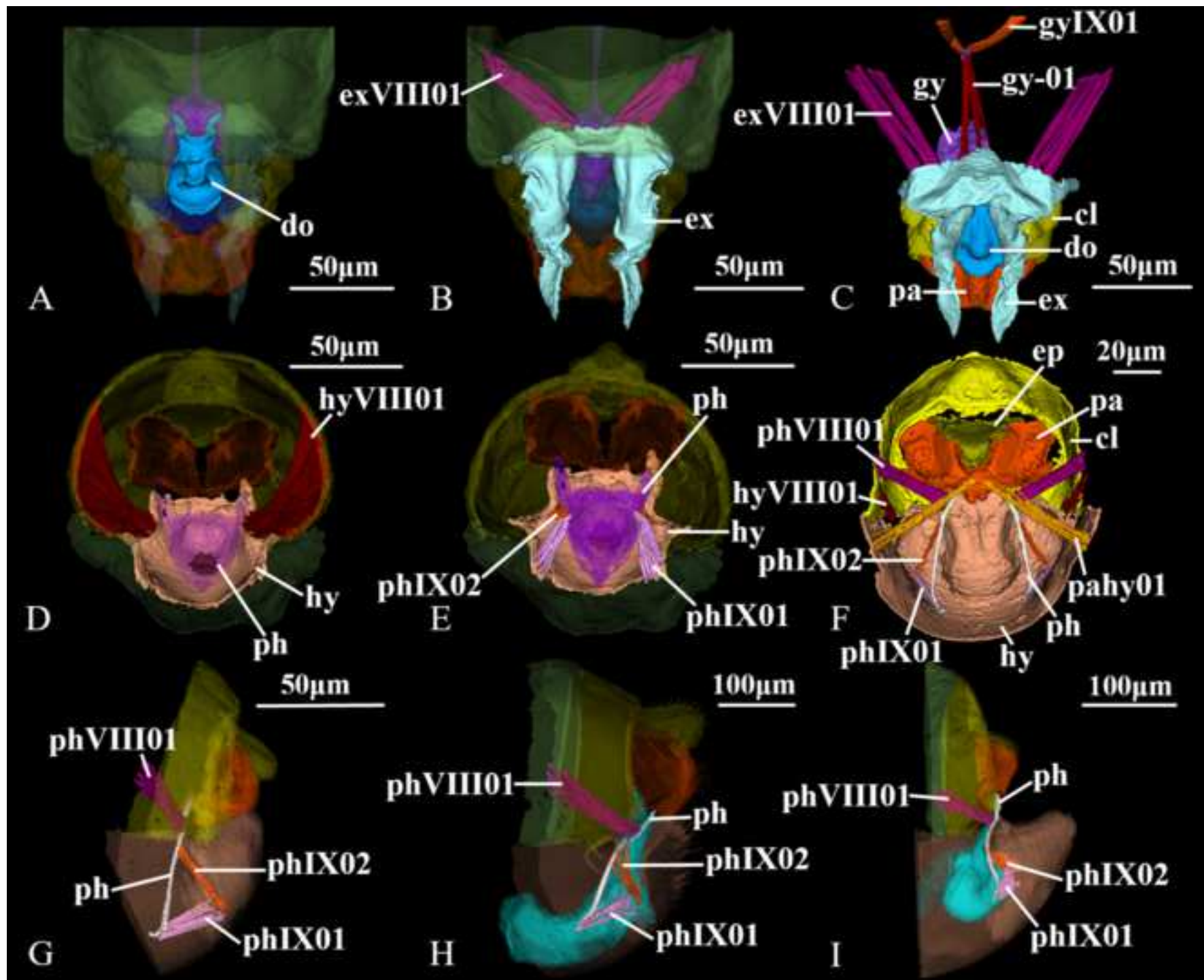




Figure 4

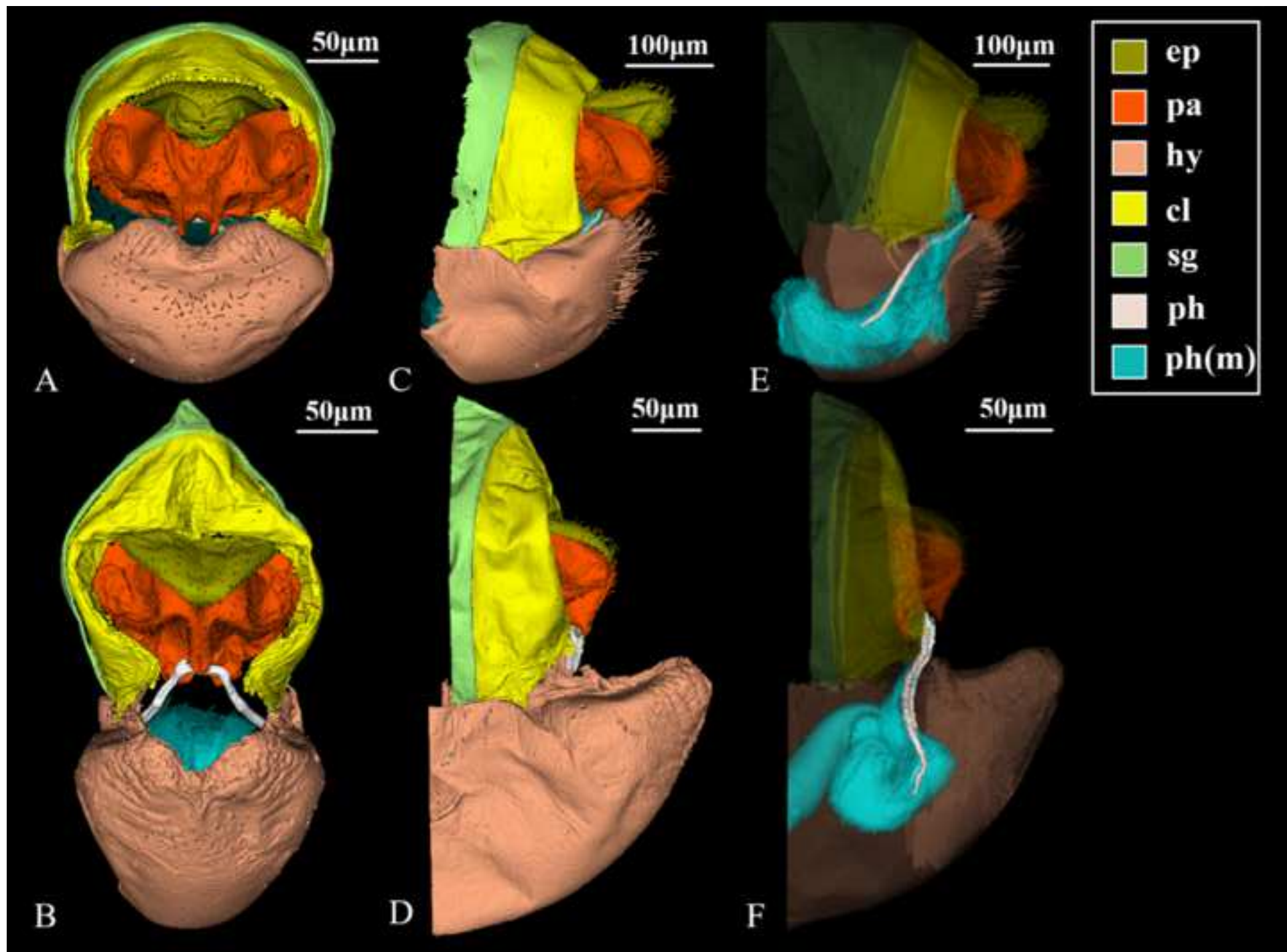


Figure 5

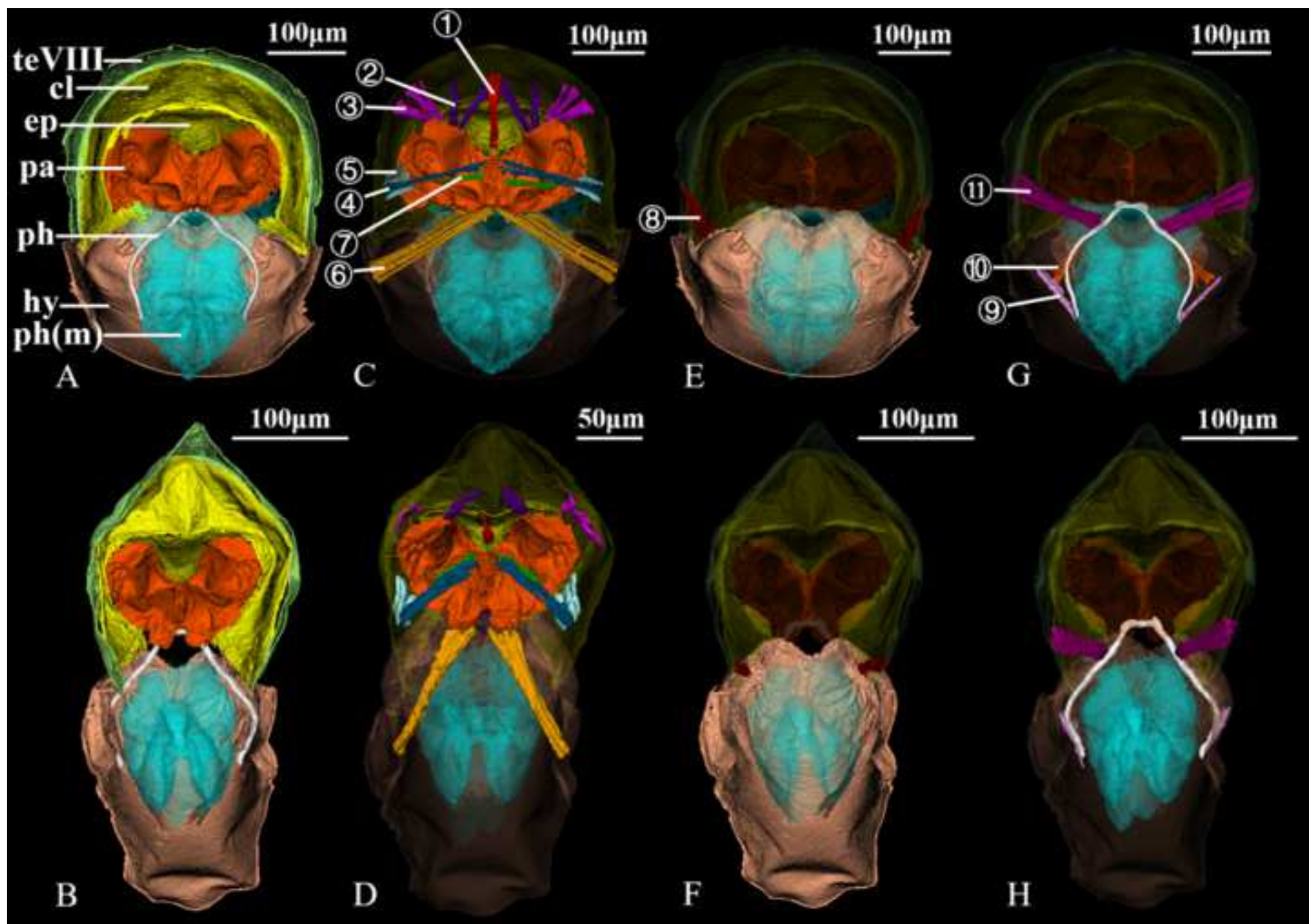


Figure 6

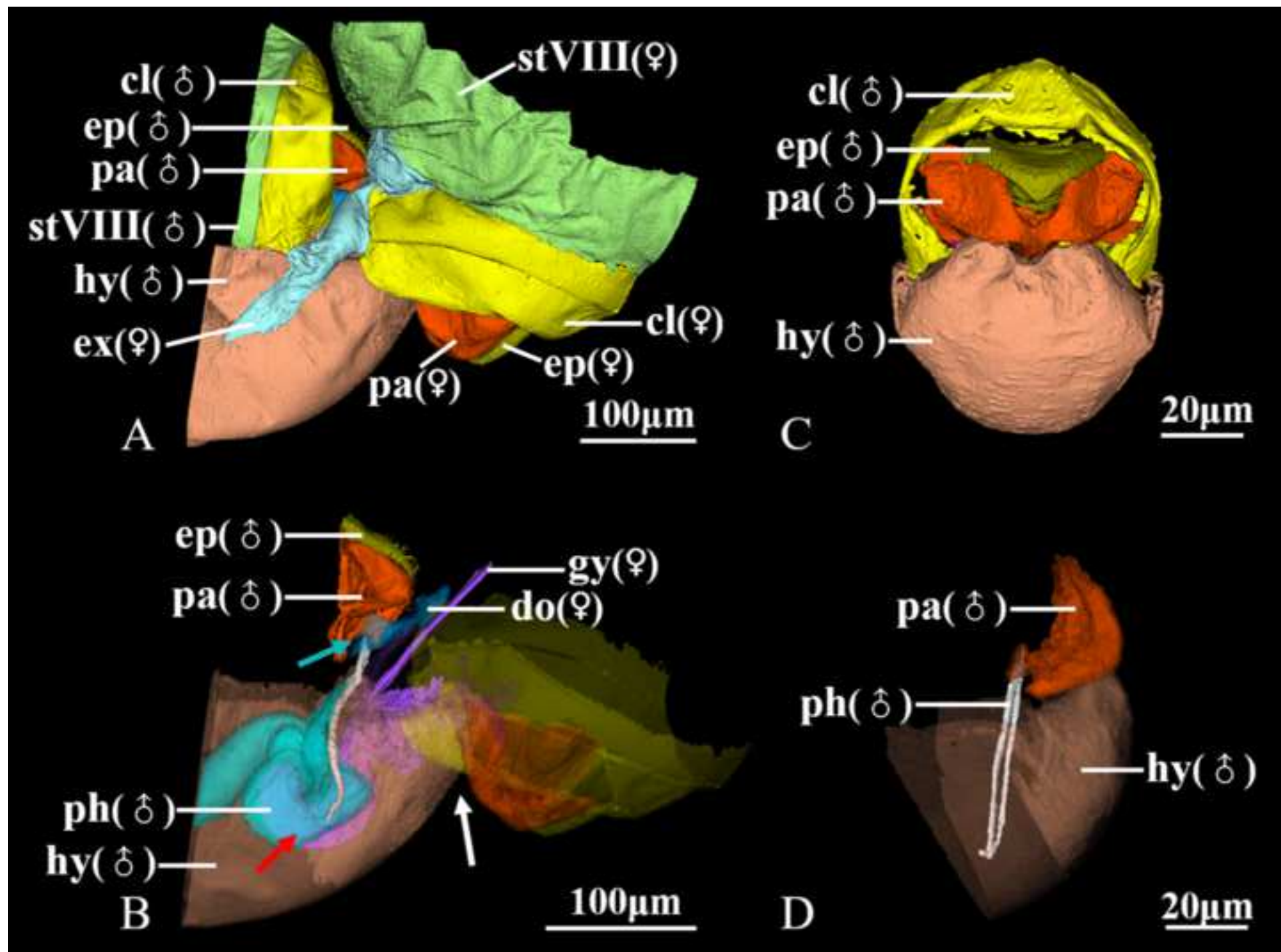


Figure 7

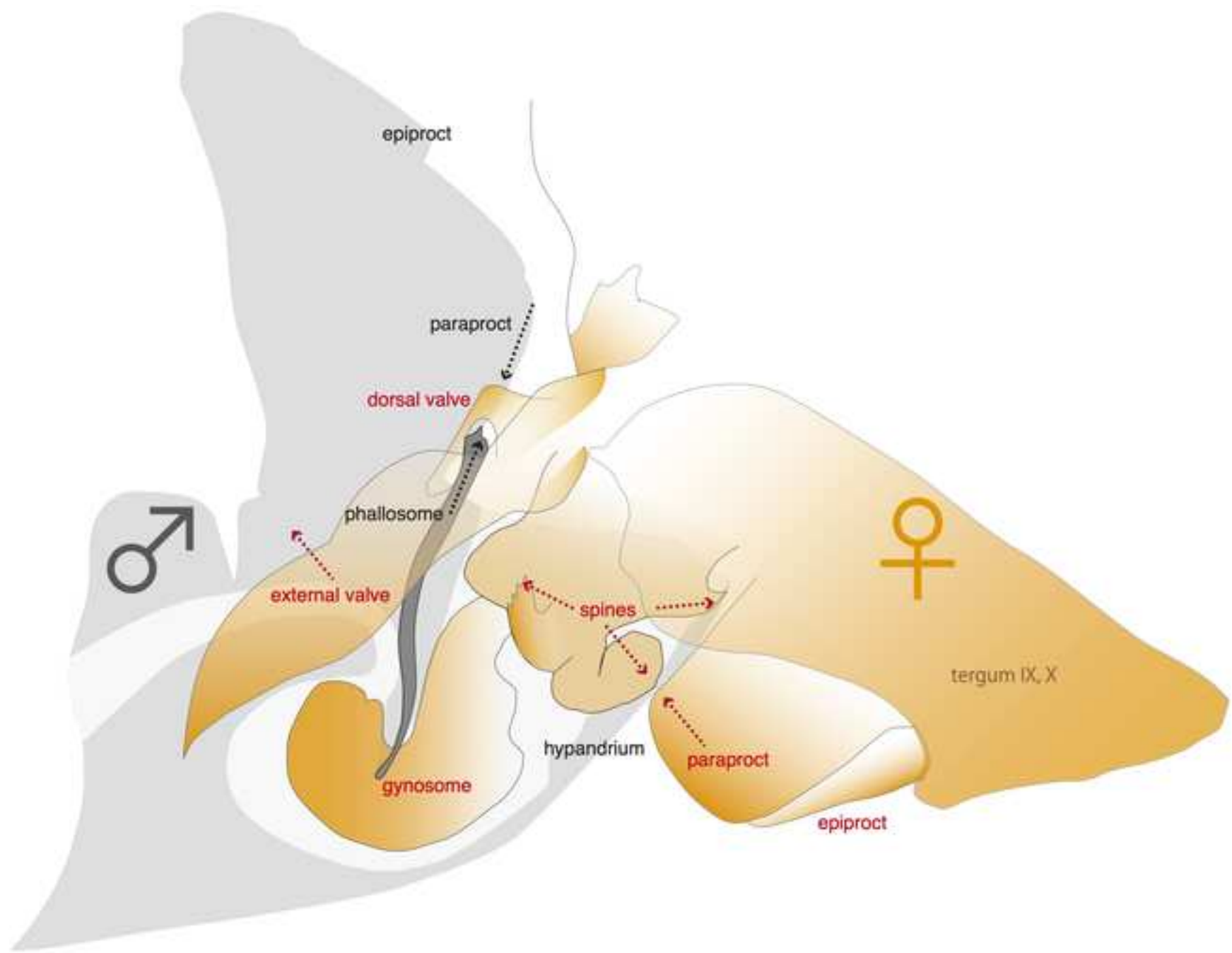


Figure 8

